Available online at www.bpasjournals.com

CFD Evaluation of Steady and Fluctuating Depth Dimpled Textures Impacting the Efficiency of Hydrodynamic Journal Bearings

Gurmeet Singh Gahir¹, Surendra Pal Singh Matharu²

^{1,2}Department of Mechanical Engineering, NIT Raipur-492010, CG, India ¹gurmeetphdwork@gmail.com, ²spsm.mech@nitrr.ac.in

How to cite this article: Gurmeet Singh Gahir, Surendra Pal Singh Matharu (2024). CFD Evaluation of Steady and Fluctuating Depth Dimpled Textures Impacting the Efficiency of Hydrodynamic Journal Bearings. *Library Progress International*, 44(3), 13814-13829.

Abstract

In this study, the impact of surface texturing on the performance of hydrodynamic journal bearings is analyzed. The theoretical evaluation are focused on various parameters including maximum pressure, load-bearing capacity, frictional force, and the coefficient of friction. A computational fluid dynamics (CFD) platform is used to design the model where the relationship between maximum pressure and the rotational angle of the shaft periphery is analyzed. Dimples are found to significantly affect the maximum pressure profile. ANSYS Fluent is utilized to simulate the journal bearing, with the shaft diameter set at 50 mm and the dimple width kept constant at 4 mm. The application of dimples resulted in an increase in lubrication film thickness. The study examined the impact of varying dimple depth profiles as well as varying dimple depthson the bearing surface. Strategically placing dimples in areas of minimum lubricant film thickness enhances the film thickness and redu ces frictional losses. Overall, the results emphasize the crucial role of dimple dimensions and placement in the pe rformance of journal bearing surfaces. The outcome revealed that applying dimples with specific depths in the region of minimum film thickness can be beneficial, suggesting potential applications of this technique in various industrial machinery.

Keywords: Coefficient of Friction, Computational Fluid Dynamics (CFD), Dimples, Frictional Force, Journal Bearing, Load bearing Capacity, Surface texture

1. 1. Introduction

In heavy machinery, rotating shafts are supported by journal bearings, which are considered crucial components for smooth functioning. These bearings require extensive lubrication to withstand severe torque and loading conditions. This need for lubrication leads to abrasive behavior of the shaft, making hydrodynamic journal bearings a very effective and common solution for supporting rotating shafts. Hydrodynamic journal bearings are simpler compared to other mechanisms like hydrostatic lifts.

Viscosity plays a critical role in hydrodynamic lubrication, directly affecting the stickiness at the interface between the shaft and bearing. Temperature variations impact viscosity, with increases in temperature leading to a decline in viscosity, and decreases in temperature causing viscosity to increase. Squeezing of the lubricant occurs due to the sliding contact between shaft and bearing surfaces. The dimple region acts as a pump for the lubricant. As the rotating speed of the journal increases, a wedge action occurs, resulting in the separation of the journal from the bearing surface. Viscosity is crucial because if it is too low, the wedge cannot form, and if it is too high, it can cause the bearing to overheat.

Over the years, many experiments have been conducted to reduce friction in journal bearings. Reducing the coefficient of friction can be accomplished by implementing appropriate textures or dimp les in regions of peak hydrodynamic pressure for bearings with a high eccentricity ratio. For bearings with a low

s [5], and the dimensions of water-

bearing

eccentricity ratio, placing these textures or dimples just downstream, where the oil/grease film thickness is at its maximum, achieves the same effect [1]. The bearingload-carrying capacity can be improved by introducing micro-patterned surfaces [2]. Additionally, analyses have shown that the pressures of closed pockets in bearings can significantly reduce the bearing friction coefficient [3]. Examination on oil-lubricated spiral-grooved journal bearings has primarily focused on cavitation occurrence, employing the "equivalent flow model" to integrate cavitation into hydrodynamic lubrication theory through a finite difference treatment of the Reynolds equation for grooved geometries [4]. References encompass factors like elastic deformation in composite journal bearings under various condition

lubricated plain journal bearings across different loads and speeds, considering elastic deformation and cavitation effects [5]. Research comparing dimple shapes found triangular dimples outperform circular ones in hydrodynamic performance [6]. Numerical analysis indicated that larger dimple diameters and smaller spacing can enhance load-carrying capacity and reduce frictional force [7]. Studies on attitude angles of dimples suggest increasing the angle enhances load support [8], while starting angles affect hydrodynamic performance positively [9].

Dimples on journal bearing surfaces have attracted interest for enhancing functionality, yet design factors like depth, attitude and starting angle, and span remain understudied [10]. Surface texturing in tribology has seen widespread use for reducing friction and wear, with numerical methods advancing the understanding of multiscale textures' lubricated behavior [11]. Laser surface texturing (LST) improves machine element tribology, notably in wear reduction and tribo-film formation, despite initial concerns over increased roughness [12]. In fluid film bearing analysis, inlet temperature profoundly influences performance modeling, aided by CFD tools for studying lubricant flow and system dynamics [13].

Utilizing ANSYS FLUENT computational fluid dynamics (CFD) software enabled the creation of an extensive model to simulate single-phase oil flow in a deep groove ball bearing (DGBB). This CFD model was instrumental in examining fluid flow characteristics influenced by bearing geometry and operating conditions. Parametric studies were conducted to determine techniques of meshing, density of meshing, and clearances in geometry, with streamlines, velocity vectors, and pressure contours employed to analyze factors such asdesign of cage and properties of lubricants specific to DGBBs [14]. Research on groove structure parameters and bearing motions discussed their influence on guiding performance, validating the design through experimental verification. Grooved bearings demonstrated lower temperature rises compared to conventional bearings, underscoring the enhancement in bearing lubrication afforded by groove structures [15]. The simulation employed the full three-dimensional Navier-Stokes equations to model steadystate flow within hydrostatic pockets, using an incompressible Newtonian fluid. Velocity vectors, streamline maps, and pressure Patterns were assessed qualitatively against experimental flow data for shallow and deep pocket types [16]. A dynamic mesh approach integrated adjacent construction influences into a comprehensive

The flow fields generated by this model were applied to a simplified single bearing chamber model in a rotating reference frame, facilitating accurate calculations of hydraulic losses while maintaining reasonable simulation ti mes. Comparative analysis of flow fields and hydraulic losses across bearing elements was conducted [17]. Investigations into load-carrying capacity highlighted improvements achieved by reducing cavitation pressure, particularly significant in lightly loaded cavitated bearings. While the Reynolds model accurately predicts leakage in non-cavitated and heavily loaded cases, its application to intermediate cavitation cases requires careful evaluation compared to JFO theory [18]. A complex numerical model validated against experimental data incorporated essential design parameters like grooves and feed holes to optimize oil distribution across the bearing gap. The study emphasized the impact of these parameters and variations in additional supply flow rates through feed holes on cavitation effects, presenting detailed three-dimensional (3-D) flow structures and cavitation regions within the bearing flow film [19].

Several studies investigated polymer composite materials for their friction characteristics at the onset of sliding, revealing PTFE-based materials as significantly outperforming traditional Babbitt metal. Testing extended

model.

to a tilting pad journal bearing test rig, highlighting dynamic characteristics influenced by bearing pad material changes and demonstrating potential performance enhancements through new lubricants, materials, and operational adjustments [20]. The journal bearing was designed using ANSYS software, modeling the journal as a "moving wall." An analytical model based on different formulas was developed for infinitely long journal bearings to determine steady-state characteristics, validated against ANSYS Computational Fluid Dynamics and Fluid-Structure Interaction simulations, which provided nearly identical solutions for L/D=1.5 journal bearings [21]. A new transient computational fluid dynamics and fluid-structure interaction approach was utilized to examine the performance of journal bearings under thermal and cavitation effects, offering insights into bearing behavior with different lubricants and serving as a reference for bearing design and substitution in varied lubrication conditions [22]. Pressure distribution obtained from Navier-Stokes equations was utilized to calculate forces and stress by resolving equations and relations. Assuming laminar and steady flow with CASTOR oil as the fluid at 3000 rpm, CFD analysis provided a pressure profile for the journal bearing: 58092.15, 58212.35, 59162.68, and 59592.64 N/m² [23].

The study employs two numerical techniques: the finite volume method for analyzing pressure, temperature, and velocity distributions in the fluid film, and the finite element method to calculate radial displacement fields. Computational Fluid Dynamics and Fluid-Structure Interaction simulations were employed to assess the impact of operational conditions on these parameters, yielding results consistent with existing literature [24]. This research focuses on factors influencing hydrodynamic journal bearing performance. The Brinkman model (BM) notably enhances lubrication efficiency in long, flexible, porous bearings compared to the Darcy model. It was observed that increasing surface roughness reduces load-carrying capacity and misalignment moment across all eccentricity ratios, while attitude angle and end leakage flow increase with roughness [25]. The paper provides a static and dynamic analysis of hydrodynamic journal bearings utilizing nano lubricants, emphasizing how the incorporation of nanoparticles affects the viscosity and performance characteristics of the lubricant. To compute pressure distribution within the bearing clearance space, employing iterative finite element methods modified Reynolds equation is utilized [26]. Furthermore, the study examines how partially textured surfaces influence the pressure distribution and load-carrying capacity of long hydrodynamic journal bearings. Utilizing the governing Reynolds equation, formulas for pressure distribution and load carrying capacity were developed, highlighting the beneficial effects of partial surface texturing on bearing performance [27]. Finally, the research introduces an integrated methodology based on Raimondi and Boyd charts and tables for designing full 360-degree hydrodynamic journal bearings. This method incorporates a rule-based production system to optimize bearing design parameters, ensuring maximum load capacity and minimal friction, thus reducing design time and errors [28]. The effect of surface roughness on hydrodynamic pressure in textured surfaces is significant, with load carrying capacity decreasing as roughness ratio increases due to the suppression of dimple-induced hydrodynamic effects. Minimizing surface roughness is crucial to enhance hydrodynamic lubrication effectiveness. A precise model was formulated to accurately assess the effect of roughness on hydrodynamic pressure [29]. The depth and width of dimples significantly influence load capacity by enhancing positive pressure distribution along the liner wall. Compared to an untextured surface with a high coefficient of friction (COF) of 39.29, textured surfaces with dimples demonstrate improved pressure generation, thereby reducing COF significantly. This stark contrast underscores the role of dimples in friction reduction [30].

Currently, it is imperative to conduct comprehensive studies on the frictional force and load-carrying capacity of journal bearings featuring dimples, with a specific focus on key design parameters such as dimple depth. Understanding how variations in dimple depth affect the tribological behavior of journal bearings, while maintaining a constant dimple width, is crucial. Moreover, assessing the influence of dimple depth on the formation and maintenance of the lubrication film, as well as its impact on hydrodynamic pressure and load-bearing capacity, is essential. To optimize the frictional force and load-carrying capability of journal bearings, considering the constraints of manufacturing processes and practical applications, it is essential to determine the ideal dimple depth. Additionally, investigating the interaction effects among different design factors and their collective impact on the tribological behavior of journal bearings with dimples will provide a comprehensive understanding. This study aims to address these knowledge gaps and provide insights into optimizing journal bearings with dimples for various applications.

2. 2. Journal Bearing Design and Analysis

2.1 2.1FEA Analysis

The hydrodynamic journal bearing is a critical component in industrial machinery, and its failure can lead to costly breakdowns and production losses. Enhancing the bearing's design is essential to extend its lifecycle and prevent such failures. Over time and under heavy loads, journal bearings are susceptible to wear, which can be mitigated by reducing the coefficient of friction—a key factor governed by frictional force. "The primary aim of this study is to reduce frictional force by investigating different dimple configurations and patterns on the internal circumference of the bearing. However, altering the bearing's surface may inadvertently decrease its load-carrying capacity, which is undesirable. Therefore, the challenge lies in identifying the optimal dimple configuration that minimizes frictional force while minimizing the reduction in load-carrying capacity.

Geometric modeling of the hydrodynamic journal bearing in ANSYS involves creating a detailed 3D representation of its geometry, encompassing parameters such as the journal's shape, dimensions, and other pertinent features as represented in Figure 1. The dimensions of the bearing used in this study align with those specified, as detailed in Table 1.

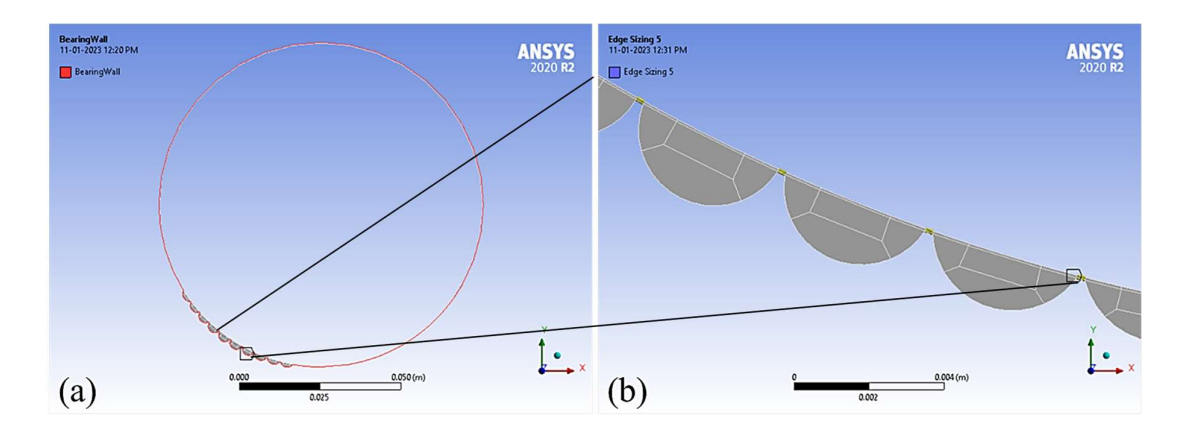


Figure 1. CAD modeling of journal bearing.

Table 1. Flood Bearing Dimensions

Parameter	Dimension
Length of bearing, l	0.133m
Shaft radius, R _s	0.05m
Radial clearance, c	0.145mm
Eccentricity ratio, ε	0.61
Attitude Angle φ	42.8°

The eccentricity of the shaft and the bearing are evaluated by using the Eq (1), where, ε is the eccentricity ratio, c is the radial clearance, and E is the eccentricity. Utilizing the values provide in Table 1, E is obtained as 0.08845 mm.

$$\varepsilon = \frac{E}{c} \tag{1}$$

The same dimensions are used to validate the methodology of the model. Each component of the geometry is assigned a name, such as the bearing surface, shaft surface, and lubrication system. Meshing is a critical step in simulating a hydrodynamic journal bearing using ANSYS or similar computational analysis software. It involves

dividing the complex geometry of the bearing into smaller, manageable elements (mesh elements or cells) for the solver to process. This discretization allows numerical computations to be performed on a finite set of points, ensuring computational feasibility. Prior to meshing, it is crucial to have a well-defined and clean geometry of the hydrodynamic journal bearing. Extraneous details should be removed, and surfaces properly defined. ANSYS offers meshing tools capable of generating various types of meshes, including structured, unstructured, and hybrid options. The meshing process subdivides the bearing's geometry into smaller elements, which can be tetrahedral, hexahedral, prismatic, other types based on the chosen Securing accurate and dependable simulation outcomes necessitates a high-quality mesh.Quality of mesh quality is determined by characteristics such as element shape, size, and distribution. Poorly generated meshes can lead to convergence issues, inaccuracies in results, and increased computation time. Figure 2 illustrates the meshed view of the bearing model.

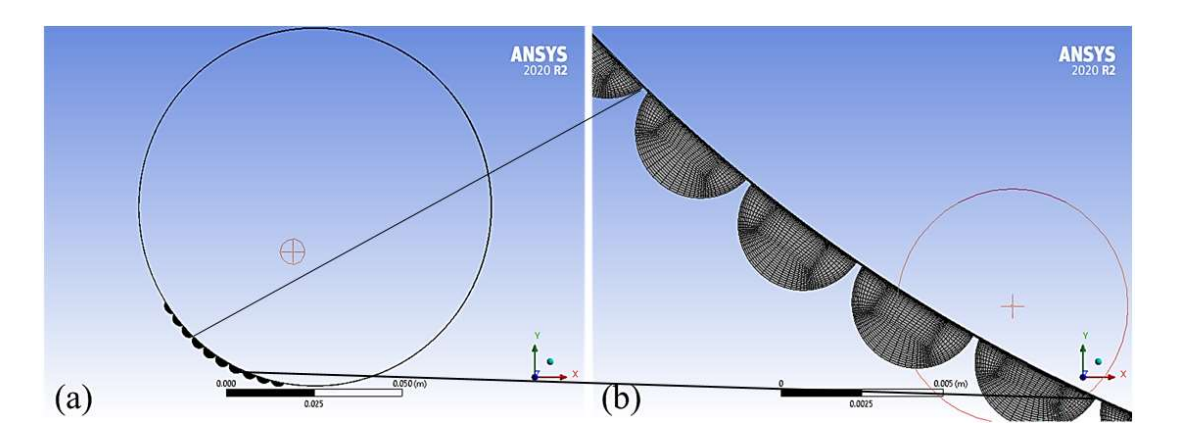


Figure 2. Meshed model of journal bearing having surface dimples.

Under the Cell Zone Conditions menu, the oil film phase is defined as a mixture with fluid type specified, and operational conditions were input during setup. The bearing wall is set stationary to simulate wall motion and configured with a no-slip condition for shear. The wallof shaft next to the bearing functions as a moving wall with rotational motion. The rotational axis origin is offset relative to the bearing center, specifically at $x = -0.0601 \, mm$ and $y = -0.0649 \, mm$. The angular speed is maintained at $48.1 \, rad/sec$ in a clockwise direction. Additionally, the shaft wall is set with a no-slip condition for shear.

2.2 2.1 Theoretical Analysis

The formula utilized for evaluating the load carrying capacity (W) is provided in Eq (2). Here, p is the maximum pressure and r is the radius of bearing.

$$W = \sqrt{\left(\int_{-\frac{l}{2}}^{\frac{l}{2}} \int_{0}^{\pi} p \, r \cos\theta \, d\theta dz\right)^{2} + \left(\int_{-\frac{l}{2}}^{\frac{l}{2}} \int_{0}^{\pi} p \, r \sin\theta \, d\theta dz\right)^{2}} \tag{2}$$

On solving the Eq (2), the load carrying capacity, W, is obtained as

$$W = 2prl \tag{3}$$

Next, to evaluated the friction force (F_f) Eq (4) is utilized, here f is the coefficient of friction.

$$F_f = f \times W \tag{4}$$

As coefficient of friction, F_f , is unknown, it is calculated from Eq (5). In Eq (5), τ is the torque and R_s is the shaft radius.

$$F_f = \frac{\tau}{R_s} \tag{5}$$

From base model, the following values are considered to evaluate the theoretical parameters: p (from Case I and Case II), radius of the bearing, r as 50.145 mm, length of the bearing, l, as 133 mm, and R_s as 0.05 m, as discussed in Sections 3.2 and 3.4.

3. 3. Results and Analysis

3.1 3.1FEAResults:

3.2 Case I: For constant dimple width and varying dimple depth profile

In this sectioneight different conditions of dimple profiles are considered. The detail description of the dimple with and depth is presented in Table 2and Figures 3. The maximum pressure is displayed where the oil is moving upstream due to the minimal gap between the shaft and the bearing surface, whereas the least pressure is displayed where the gap is greatest. Figure 4 displays the variation of pressure along the different regions of the bearing (different dimple profiles). From Figure 4, the maximum pressure (*p*) attained for all the eight cases, respectively, are as follows:2.200E+05 *Pa*, 2.35 E+05 *Pa*, 2.375 E+05 *Pa*, 2.164E+05 *Pa*, 2.192E+05 *Pa*, 2.190E+05 *Pa*, 2.135E+05 *Pa*, and 2.149E+05 *Pa*.

Table 2. Different dimple profiles (Case I-1 to I-8).

Different Dimple Profiles	Dimple Width	Dimple Depth	
Case I-1	Constant	Constant	
Case I-2	Constant	Decreasing	
Case I-3	Constant	Increasing	
Case I-4	Constant	Initial Increasing then Decreasing	
Case I-5	Constant	Initial Decreasing then Increasing	
Case I-6	Constant	Alternate Maximum-Minimum	
Case I-7	Constant	Alternate Minimum-Maximum	
		(Lower depth in comparison to CaseI-6 and	
		Case I-8)	
Case I-8	Constant	Alternate Minimum-Maximum	

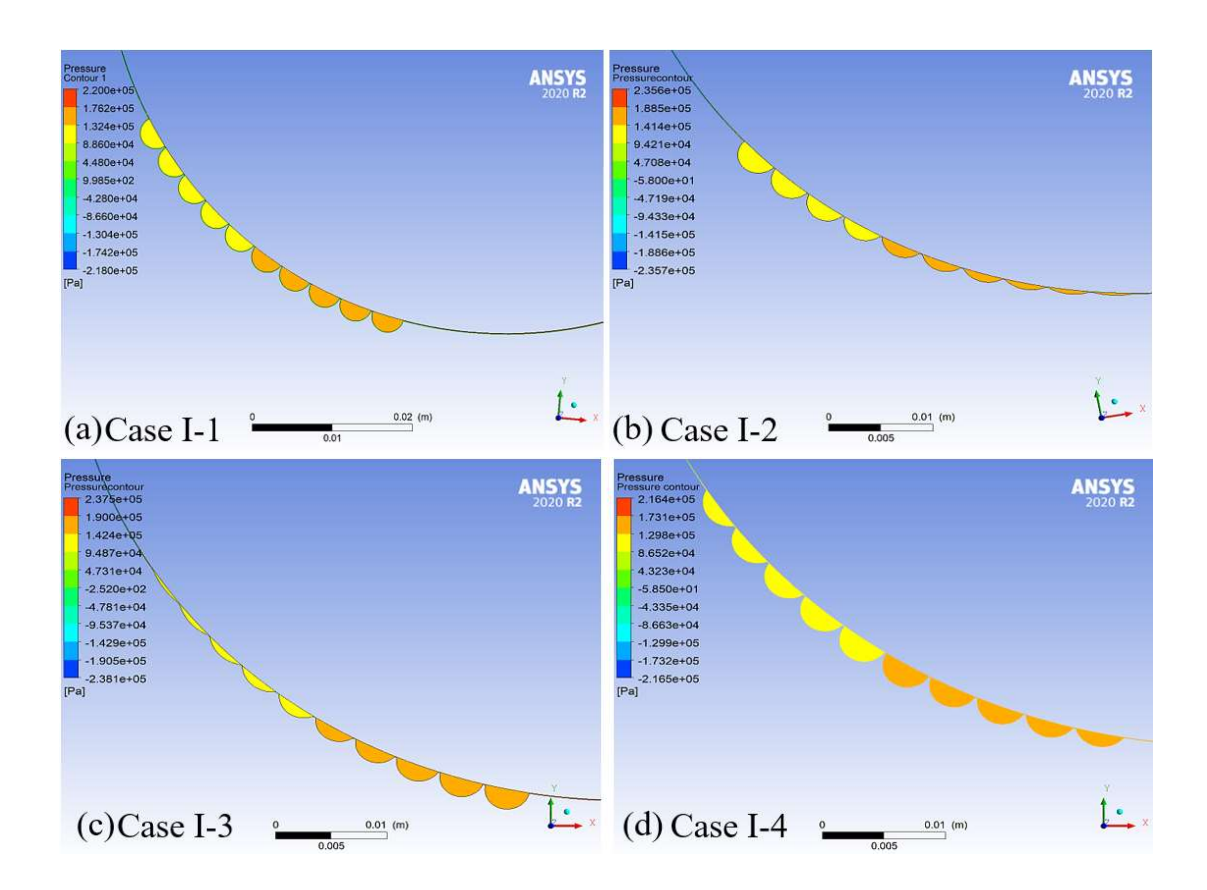


Figure 3. Pressure contour distribution under various dimple profiles (Case I):(a)Case I-1,(b) Case I-2, (c) Case I-3, and (d) Case I-4.

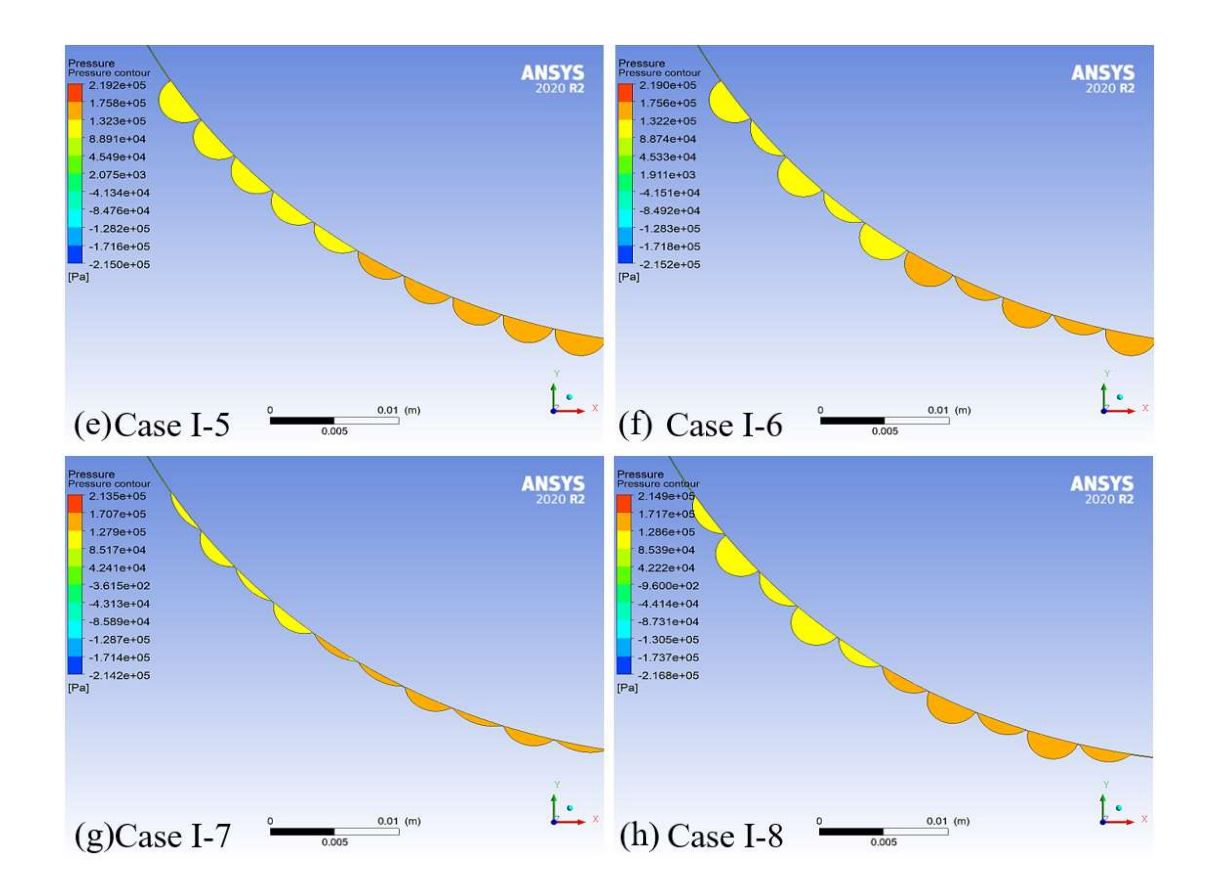


Figure 3 (Continue). Pressure contour distribution under various dimple profiles (Case I):(e)Case I-5,(f) Case I-6, (g) Case I-7, and (h) Case I-8.

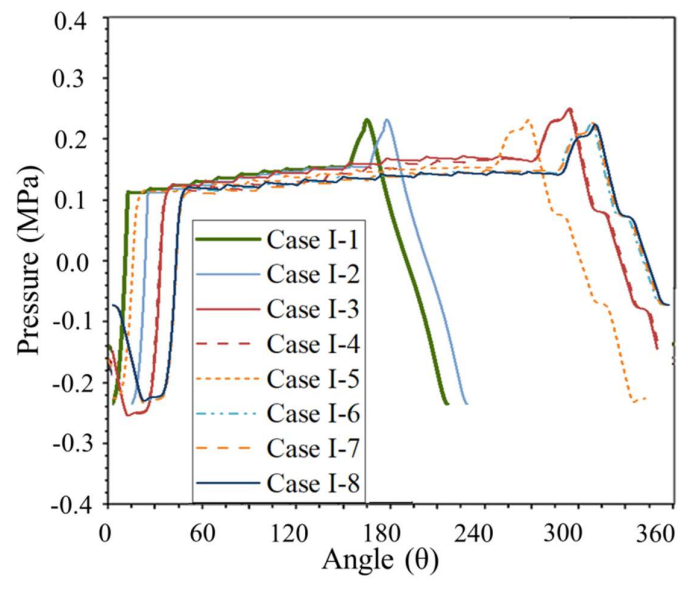


Figure 4. Pressure variation along different dimple depth profiles.

3.3 3.2Theoretical Results: Case I: For constant dimple width and varying dimple depth profile

From the analysis, the obtained values of torque for different pressures are presented in Table 3. The evaluated values for all the targeted Cases I are presented in Table 3.

Table 3. Evaluated values for different dimple profiles (Case I-1 to I-8).

Different Dimple Profiles	Maximum pressure, p (MPa)	Load Carrying Capacity, W (N)	Friction Force, F _f (N)	Coefficient of Friction, f
Case I-1	0.22	2934.49	45.19	0.015
Case I-2	0.2356	3142.57	45.46	0.014
Case I-3	0.237	3161.24	45.56	0.014
Case I-4	0.2164	2886.47	46.02	0.016
Case I-5	0.2192	2923.81	46.09	0.016
Case I-6	0.219	2921.15	46.21	0.016
Case I-7	0.2135	2847.78	48.95	0.017
Case I-8	0.2149	2866.46	46.51	0.016

3.4 3.3FEAResults: Case II: For constant dimple width and different dimple depth

In this section ten different conditions of dimple profiles are considered. The detail description of the dimple with and depth is presented in Table 4and Figures5.

Table 4. Different dimple depths (Case II-1 to II-10).

Different Dimple Profiles	Dimple Width	Dimple Depth (mm)
Case II-1	Constant	0.25
Case II-2	Constant	0.50
Case II-3	Constant	0.75
Case II-4	Constant	1.00
Case II-5	Constant	1.25
Case II-6	Constant	1.50
Case II-7	Constant	1.75
Case II-8	Constant	2.00
Case II-9	Constant	2.25
Case II-10	Constant	2.50

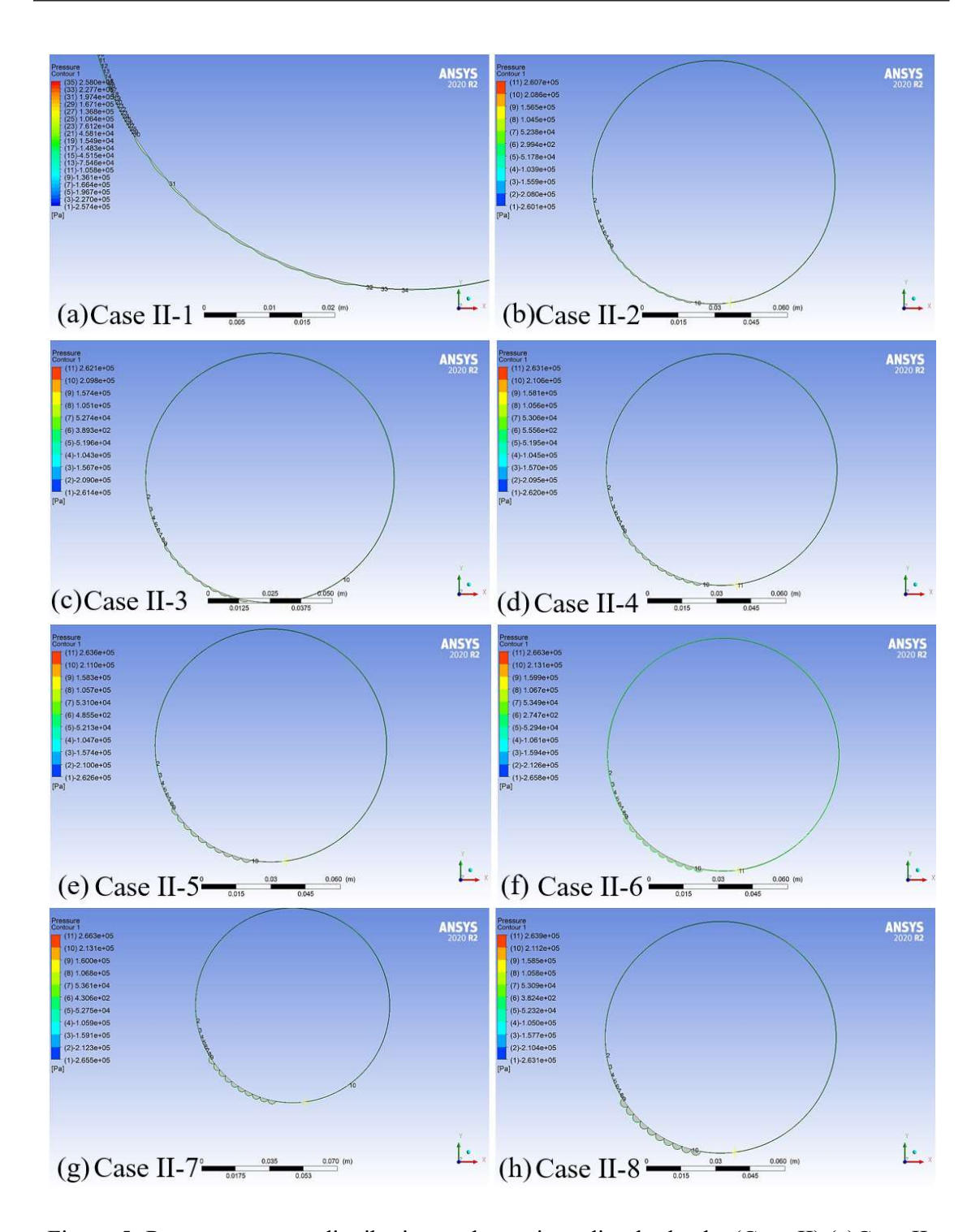


Figure 5. Pressure contour distribution under various dimple depths (Case II):(a)Case II-1,(b) Case II-2, (c) Case II-3, (d) Case II-4, (e)Case II-5,(f) Case II-6, (g) Case II-7, and (h) Case II-8.

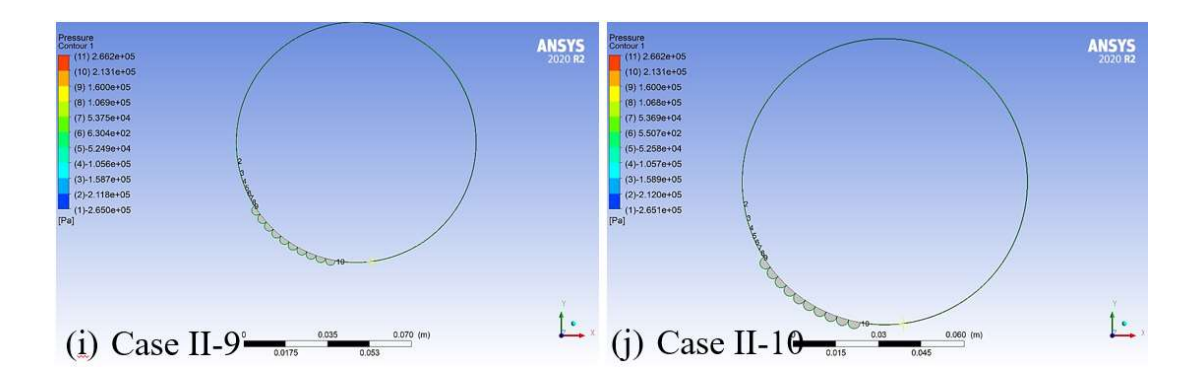


Figure 5 (Continue). Pressure contour distribution under various dimple profiles (Case II):(i)Case II-9,(j) Case II-10.

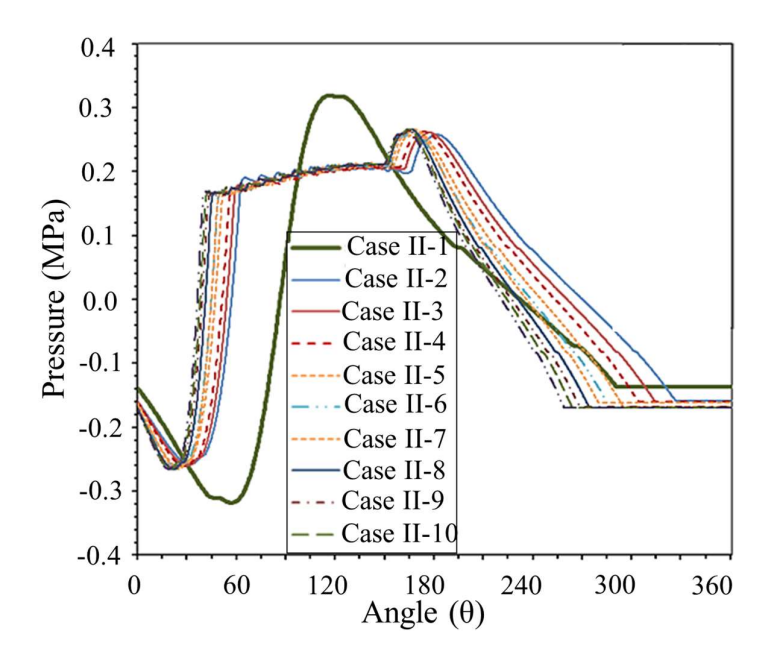


Figure 6. Pressure variation along different dimple depths.

3.5 3.4 Theoretical Results: Case II: For constant dimple width and different dimple depth

From the analysis, the obtained values of torque for different pressures are presented in Table 5. Also, the evaluated values for all the targeted Cases II are depicted in Table 5.

Table 5.	Evaluated	values to	r different	dimple	depths (Case II-	1 to II-10).
----------	-----------	-----------	-------------	--------	----------	----------	--------------

Different Dimple Profiles	Maximum pressure, p (MPa)	Load Carrying Capacity, W (N)	Friction Force, F _f (N)	Coefficient of Friction, f
Case II-1	0.258	3441.35	47.18	0.014
Case II-2	0.2607	3477.37	44.39	0.013
Case II-3	0.2621	3496.04	42.84	0.012
Case II-4	0.2631	3509.38	41.95	0.012
Case II-5	0.2636	3516.05	41.38	0.012
Case II-6	0.2663	3552.06	40.78	0.011
Case II-7	0.2663	3552.06	40.56	0.011
Case II-8	0.2639	3520.05	40.64	0.012
Case II-9	0.2662	3550.73	40.25	0.011
Case II-10	0.2662	3550.73	40.11	0.011

3.6 3.5 Comparative Results: FEA and Theoretical

The results of the various conditions as shown in Fig. a – Fig. c along with a comparison to our reference model. And it is abundantly clear from the above table that the configurations we selected for our dimples resulted in a decrease in load carrying capacity while increasing the frictional force on the shaft. When we considered both of these factors, we obtained a noticeably higher percentage of increase in the bearing's coefficient of friction. As we all know, if there is a high coefficient of friction between two surfaces, it indicates that there is a strong resistance to relative motion between those surfaces. This means that the surfaces in touch will experience more wear and tear over time, which will eventually cause damage.

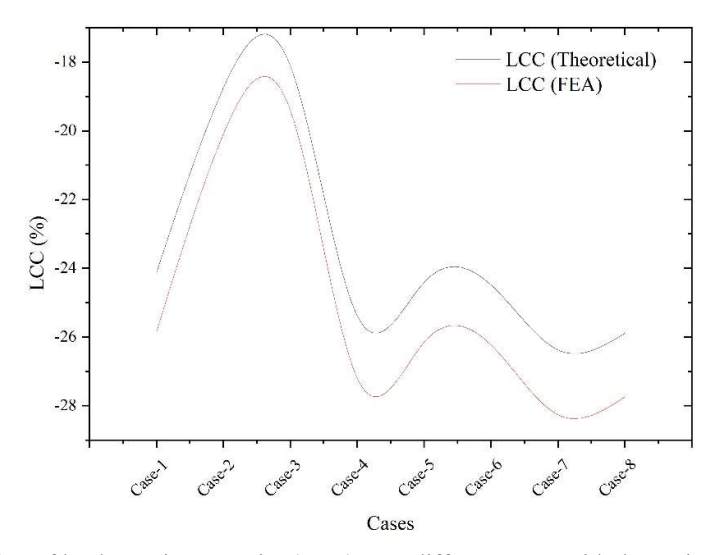


Figure a. Variation of load carrying capacity (LCC) over different cases with theoretically and FEA results

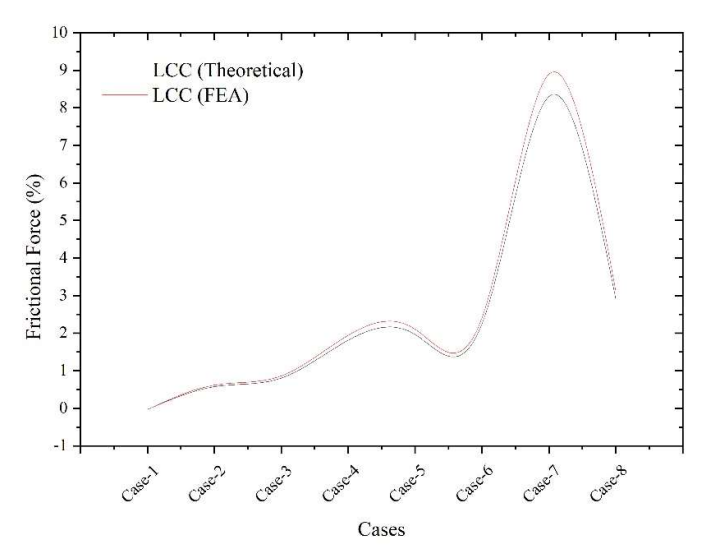


Figure b. Variation of frictional force over different cases with theoretically and FEA results

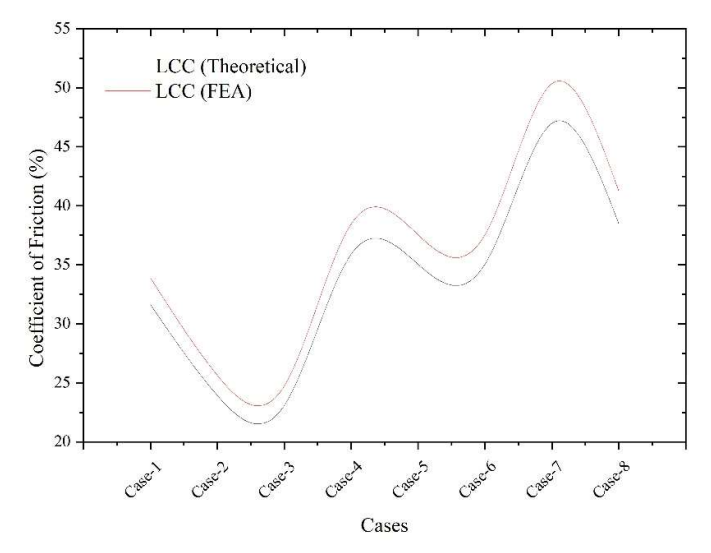


Figure c. Variation of coefficient of friction over different cases with theoretically and FEA results Now, further changes have been applied with again various cases, the depth of the dimple and conducted several experiments with various dimple configurations because the results were not in our favor. The results are presented below Fig. d-Fig. f:

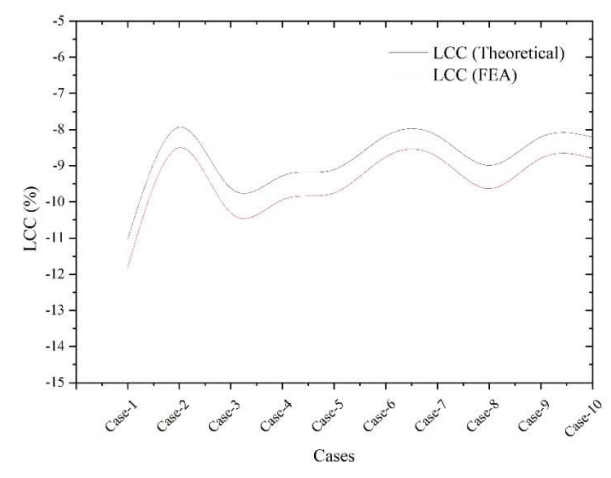


Figure d. Variation of load carrying capacity (LCC) over different cases with theoretically and FEA results

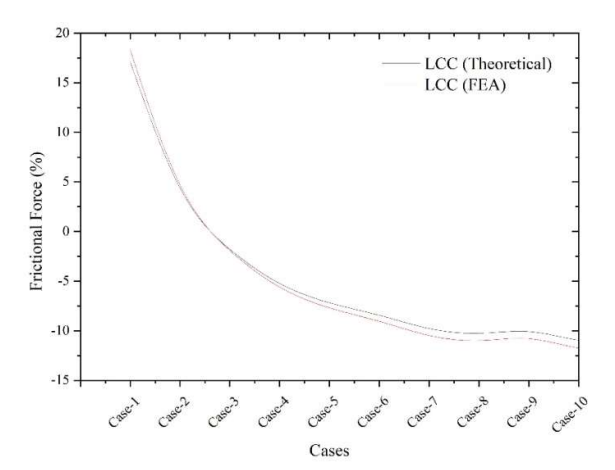


Figure e. Variation of frictional force over different cases with theoretically and FEA results

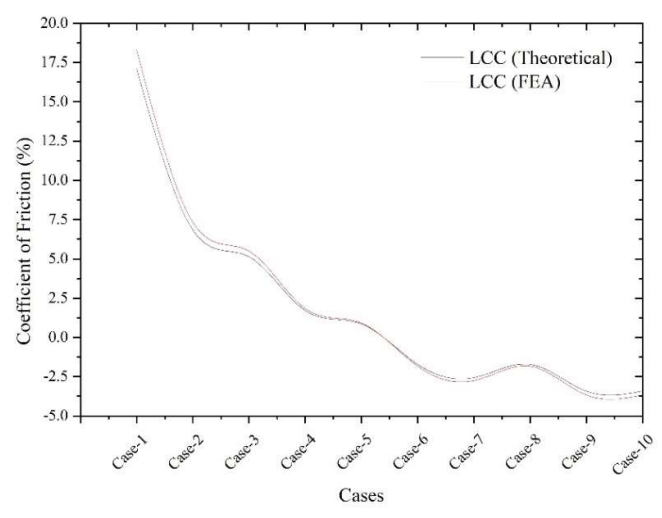


Figure f. Variation of coefficient of friction over different cases with theoretically and FEA results As can be seen in the figures, when we compare all of the experiment's percentage-wise to our base model, we discovered that as we increased the depth of the dimples, the load carrying capacity, the bearingfrictional force, and the coefficient of friction all decreased. As seen in the above table, trials with dimple depths of 1.5 mm and

higher have produced positive outcomes. When comparing all the data, dimples with a depth of 2.25 mm have produced the greatest results among all configurations due to their second-lowest percentage loss in terms of load bearing capacity, second-lowest frictional force, and lowest drop in coefficient of friction

4. 4. Conclusion

The analysis of the load-carrying capability of textured bearings with dimples of variable and constant depth was conducted in terms of the friction coefficient, leading to the following conclusions:

The maximum pressure is significantly reduced, resulting in a decrease in load-carrying capacity by 18% to 26%, while the coefficient of friction increases by 23% to 47% compared to bearings without dimples. Hence, bearing configurations with varying dimple depths are not successful. Dimpling on bearing surfaces impacts load capacity, with dimples having a ratio of d/hmin> 1 in the area of peak pressure at a high eccentricity ratioshowing a greater percentage drop in the coefficient of friction and a smaller reduction in load-carrying capacity. The analysis revealed that the reduction in the coefficient of friction begins at a dimple depth of 1.5 mm, with the maximum reduction observed at a dimple depth of 2.25 mm. Although the maximum pressure shifts to the fourth quadrant, just right of the dimple zone, the pressure within the dimple region remains nearly constant. Contour plots indicate that pressure increases from the region of maximum film thickness to the dimple region, with a steep pressure drop observed from the maximum pressure location to just below the cavitation zone, where pressure remains almost constant.

Based on these findings, it can be inferred that adding dimples of the ideal size and shape to the journal's minimum film thickness area at a high eccentricity ratio will enhance the hydrodynamic journal bearing's functionality. While there is a trade-off with pressure, the reduction in frictional force and the coefficient of friction can increase bearing life. Additionally, spiral grooves with various configurations, different cross-sectional shapes of dimples, and dimples in the cavitation zone could provide better results. Surface texturing with engraved and embossed shapes can also be analyzed for improved outcomes. CFD analysis can be extended to journals with variable depths and attitude angles based on the bearing's speed and load. Experimental testing is recommended to validate the analysis and achieve more accurate results in real-world conditions. Further analysis for different eccentricity ratios, affecting the minimum film thickness, can offer more opportunities for research and optimization.

5. References

- 1. Cupillard, Samuel, Michel Cervantes, and Sergei Glavatskih. "A CFD study of a finite textured journal bearing." *IAHR Symposium on Hydraulic Machinery and Systems*: 27/10/2008-31/10/2008. 2008.
- 2. Sahlin, Fredrik, et al. "Two-dimensional CFD-analysis of micro-patterned surfaces in hydrodynamic lubrication." J. Trib. 127.1 (2005): 96-102.
- 3. Brajdic-Mitidieri, Petra, et al. "CFD analysis of a low friction pocketed pad bearing." (2005): 803-812.
- 4. Hirayama, et al. "Analysis of dynamic characteristics of spiral-grooved journal bearing with considering cavitation occurrence." JSME International Journal Series C Mechanical Systems, Machine Elements and Manufacturing 48.2 (2005): 261-268.
- 5. Wang, Yanzhen, et al. "Study of the lubrication performance of water-lubricated journal bearings with CFD and FSI method." Industrial Lubrication and Tribology (2016).
- 6. Li, Hulin, et al. "Study on the performance of journal bearings in different lubricants by CFD and FSI method with thermal effect and cavitation." MATEC Web of Conferences. Vol. 249. EDP Sciences, 2018.
- 7. Hua, Xijun, et al. "Friction properties and lubrication mechanism of self-lubricating composite solid lubricant on laser textured AISI 52100 surface in sliding contact." International Journal of Surface Science and Engineering 12.3 (2018): 228-246.
- 8. Zhang, Yu, Guoding Chen, and Lin Wang. "Effects of thermal and elastic deformations on lubricating properties of the textured journal bearing." Advances in Mechanical Engineering 11.10 (2019): 1687814019883790.
- 9. Liu, Xiyao, et al. "Study on self-adaptive lubrication mechanism of surface micro-dimple structure filled with multiple lubricants." Journal of Alloys and Compounds 861 (2021): 158479.

- 10. Rahnejat, Homer, ed. *Tribology and dynamics of engine and powertrain: fundamentals, applications and future trends*. Elsevier, 2010.
- 11. Grützmacher, Philipp G. et al. "Multi-scale surface texturing in tribology—Current knowledge and future perspectives." Lubricants 7.11 (2019): 95.
- 12. Hsu, Chia-Jui, et al. "Does laser surface texturing really have a negative impact on the fatigue lifetime of mechanical components?." Friction 9 (2021): 1766-1775.
- 13. Wasilczuk, Michał, and Grzegorz Rotta. "*Modeling lubricant flow between thrust-bearing pads.*" Tribology International 41.9-10 (2008): 908-913.
- 14. Peterson, Wyatt, et al. "A CFD investigation of lubricant flow in deep groove ball bearings." Tribology International 154 (2021): 106735.
- 15. Ge, Linfeng, et al. "Design of groove structures for bearing lubrication enhancement based on the flow mechanism analysis." Tribology International 158 (2021): 106950.
- 16. Horvat, F. E., and M. J. Braun. "Comparative experimental and numerical analysis of flow and pressure fields inside deep and shallow pockets for a hydrostatic bearing." Tribology transactions 54.4 (2011): 548-567
- 17. Feldermann, Achim, et al. "Determination of hydraulic losses in radial cylindrical roller bearings using CFD simulations." Tribology International 113 (2017): 245-251.
- 18. Xu, Wanjun, et al. "Reynolds Model versus JFO Theory in Steadily Loaded Journal Bearings." Lubricants 9.11 (2021): 111.
- 19. Riedel, M., M. Schmidt, and P. Stücke. "Numerical investigation of cavitation flow in journal bearing geometry." EPJ Web of Conferences. Vol. 45. EDP Sciences, 2013.
- 20. Simmons, Gregory F. "Journal bearing design, lubrication and operation for enhanced performance". Diss. Luleåtekniskauniversitet, 2013.
- 21. Tiwari, Priyanka, and Veerendra Kumar. "*Analysis of hydrodynamic journal bearing using CFD and FSI technique*." International Journal of Engineering Research & Technology 3.7 (2014): 1210-1215.
- 22. Li, Hulin, et al. "Study on the performance of journal bearings in different lubricants by CFD and FSI method with thermal effect and cavitation." MATEC Web of Conferences. Vol. 249. EDP Sciences, 2018.
- UdgireManojkumar, N., H. Jagadish, and B. Kirankumar. "CFD analysis of hydro-dynamic lubrication journal bearing using castor oil." Recent Trends in Mechanical Engineering: Select Proceedings of ICIME 2019. Springer Singapore, 2020.
- 24. Ouadoud, A., A. Mouchtachi, and N. Boutammachte. "*Numerical simulation CFD, FSI of a hydrodynamic journal bearing.*" Journal of Advanced Research in Mechanical Engineering 2.1 (2011).
- 25. Tiwari, Priyanka, and Veerendra Kumar. "Analysis of hydrodynamic journal bearing: A review." International Journal of Engineering Research & Technology 1.7 (2012): 1-7.
- 26. Prabhakaran Nair, K., Mohammed Shabbir Ahmed, and SaedThamer Al-qahtani. "Static and dynamic analysis of hydrodynamic journal bearing operating under nano lubricants." International Journal of Nanoparticles 2.1-6 (2009): 251-262.
- 27. Hamdavi, Shahab, H. H. Ya, and N. Rao. "Effect of surface texturing on hydrodynamic performance of journal bearing." ARPN Journal of Engineering and Applied Sciences 11.1 (2016): 172-176.
- Kalani, Anand, Sandeep Soni, and Rita Jani. "Expert Knowledgebase System for Computer Aided Design of Full Hydrodynamic Journal Bearing." International Journal of Mechanical Engineering and Technology 6.8 (2015): 46-58.
- 29. Ji, Jing-Hu, Cai-Wei Guan, and Yong-Hong Fu. "Effect of micro-dimples on hydrodynamic lubrication of textured sinusoidal roughness surfaces." Chinese Journal of Mechanical Engineering 31.1 (2018): 1-8.
- 30. Ghani, Jaharah A., et al. "Computational fluid dynamic analysis on tribological performance under hydrodynamic lubrication of dimple textured surface produced using turning process." Wear 477 (2021): 203898.